

Military Technical College
Kobry El-Kobbah,
Cairo, Egypt.



15th International Conference
on Applied Mechanics and
Mechanical Engineering.

EFFECT OF SCREEN MESH WICK AND Al_2O_3 NANOFLUID CONCENTRATION ON CIRCULAR HEAT PIPE PERFORMANCE

E. A. Abdel-Hadi*, S. H. Taher ^{*}, M. G. Mousa ^{**} and S. M. Elshamy ^{***}

ABSTRACT

In this paper the experimental study of the behavior of screen wick and nanofluid to improve the performance of a circular heat pipe. Pure water and Al_2O_3 -water based nanofluid are used as working fluids. An experimental setup is designed and constructed to study the heat pipe performance under different operating conditions. The effect of filling ratio, volume fraction of nano-particle in the base fluid, screen mesh as a wick and heat input rate on the thermal resistance is investigated. Total thermal resistance of the heat pipe for pure water and Al_2O_3 -water based nanofluid is also predicted. An experimental correlation is obtained to predict the influence of Prandtl number and dimensionless heat transfer rate, K_q on thermal resistance. Thermal resistance decreases with increasing Al_2O_3 -water based nanofluid compared to that of pure water. The experimental data is compared to the available data from previous work. The range of operating parameter are filling ratio 40% to 100%, nanofluid concentration from 0.0% to 2.0%, and heat rate from 8 to 32 watt. The agreement is found to be fairly good.

KEY WORDS

Heat Pipe, Thermal Performance, Nanofluids, Wick type.

* Professor, Dpt. of Mechanical Engineering, Benha University, Shobra, Egypt.

** Associate professor, Dpt. of Mechanical Engineering, Mansoura University, Mansoura, Egypt. Email: Mgmousa@mans.edu.eg.

*** Lecturer assistant, High institute for engineering and technology, Obour, Egypt. Email: s_el_shamy@yahoo.com.

NOMENCLATURE

A	Surface area, m ²
FR	Filling ratio
I	Electric current, Amp
k	thermal conductivity, W/m.K
N	Number of thermocouples
Q	Input heat rate, W
q	Heat flux, W/m ²
R	Total thermal resistance of heat pipe, K/W
r	Electric resistance, Ω
T	Temperature, K
V	Applied voltage, Volt
X	Horizontal distance, mm

Greek Symbols

Φ	Volume fraction of nanoparticles, %
ρ	Density, kg/m ³
μ	Dynamic viscosity, N.s/m ²

Subscript

c	Condenser
e	Evaporator
ef	Effective
v	vapor
g	gravitational
l	Liquid
m	Base fluid
p	Particles

Dimensionless Numbers

RR	Reduction factor in thermal resistance $\frac{(R_m - R_{ef})}{R_m}$
----	---

K _q	Dimensionless heat transfer rate $\frac{K_{ef} \times L_e \times \Delta T}{Q}$
----------------	--

Pr	Prandtl number $\frac{\mu_{ef} \times Cp_{ef}}{K_{ef}}$
----	---

INTRODUCTION

To solve the growing problem of heat generation by electronic equipment, two-phase change devices such as heat pipe and thermosyphon cooling systems are now used in electronic industry. Heat pipes are passive devices that transport heat from a heat source to a heat sink over relatively long distances via the latent heat of vaporization

of a working fluid. The heat pipe generally consists of three sections; evaporator, adiabatic section and condenser. In the evaporator, the working fluid evaporates as it absorbs an amount of heat equivalent to the latent heat of vaporization. The working fluid vapor condenses in the condenser and then, returns back to the evaporator. Nanofluids, produced by suspending nano-particles with average sizes below 100 nm in traditional heat transfer fluids such as water and ethylene glycol provide new working fluids that can be used in heat pipes. A very small amount of guest nano-particles, when uniformly and suspended stably in host fluids, can provide dramatic improvement in working fluid thermal properties. The goal of using nanofluids is to achieve the highest possible thermal properties using the smallest possible volume fraction of the nano-particles (preferably < 1% and with particle size < 50 nm) in the host fluid.

Kyu et al.[1] study the effect of nanofluids on the thermal performance of heat pipes by testing circular screen mesh wick heat pipes using water-based Al_2O_3 nanofluids with the volume fraction of 1.0 and 3.0 Vol.%. Based on the observation, it is first shown that the primary mechanism on the enhancement of the thermal performance for the heat pipe was the coating layer formed by nanoparticles at the evaporator section because the layer can not only extend the evaporation surface with high heat transfer performance but also improve the surface wettability and capillary wicking performance.

Mousa [2] experimentally study the behavior of nanofluid to improve the performance of a circular heat pipe. Pure water and Al_2O_3 -water based nanofluid used as working fluid. An experimental setup was design and constructed to study the heat pipe performance under different operating conditions. The effect of filling ratio, volume fraction of nano-particles in the base fluid, and heat input rate on the thermal resistance was investigated. Total thermal resistance of the heat pipe for pure water and Al_2O_3 -water based nanofluid also predicted. An experimental correlation obtained to predict the influence of Prandtl number and dimensionless heat transfer rate, Kq on thermal resistance. Thermal resistance decreases with increasing Al_2O_3 -water based nanofluid compared to that of pure water. The experimental data compared to the available data from previous work. The agreement is found to be fairly good.

ZhenHua and QunZhi [3] investigate the effects of aqueous CuO nanofluids on thermal performance of a horizontal mesh heat pipe working at steady sub-atmospheric pressures. The nanofluid was composed of deionized water and CuO nanoparticles with an average diameter of 50 nm. The thermal performance of a mesh heat pipe can be evidently strengthened by substituting CuO nanofluids for deionized water under sub-atmospheric pressures. Maryam et al. [4] study the thermal performance of a cylindrical heat pipe utilizing nanofluids by a two-dimensional analysis. Three of the most common nanoparticles, namely Al_2O_3 , CuO , and TiO_2 are considered as the working fluid. The existence of an optimum mass concentration for nanoparticles in maximizing the heat transfer limit is established. The effect of particle size on the thermal performance of the heat pipe is also investigated. It is found that smaller particles have a more pronounced effect on the temperature gradient along the heat pipe. Kempers et al. [5] investigated experimentally the heat transfer mechanisms in the condenser and evaporator sections of a copper-water wicked heat pipe with 3 layers of screen mesh. A

composite heat transfer model for the heat pipe is proposed that considers both conduction and boiling heat transfer in the evaporator.

Zhen et al. [6] study the heat transfer performance of a cylindrically micro-grooved heat pipe using aqueous nanofluids as the working fluids. The base liquid was distilled water, while, the five kinds of nanoparticles. The heat transfer performance. The main reason that causes these differences in the heat transfer performance results from the surface structure of the coating layer formed by sediment of nanoparticles on the heated surface. Zeinali Heris et al. [7] investigate experimentally laminar flow forced convection heat transfer of Al_2O_3 /water nanofluid inside a circular tube with constant wall temperature. The Nusselt numbers of nanofluids were obtained for deferent nanoparticle concentrations as well as various Peclet and Reynolds numbers. Experimental results emphasize the enhancement of heat transfer due to the nanoparticles presence in the fluid. Heat transfer coefficient increases by increasing the concentration of nanoparticles in nanofluid. The increase in heat transfer coefficient due to presence of nanoparticles is much higher than the prediction of single phase heat transfer correlation used with nanofluid properties.

Wei et al. [8] Investigate thermal resistance of pure water and nanofluid filled heat pipes. Nanofluid is employed as working medium for conventional 200 μm wide grooved circular heat pipe. The nanofluid used is an aqueous solution of various-solution silver (Ag) nanoparticles. The average diameters of Ag nanoparticles are 10 nm. At the same charge volume of 0.45mL, test result showed the average decrease of 30%-70% in thermal resistance of heat pipe with nanofluid as compared with pure water. Chen [9] studied the effect of various concentrations on flat heat pipe thermal performance by air-cooling testing equipment. The particles used in these experiments were silver particles 35 nm in size. The base working fluid was pure-water. Nano-fluids were prepared using a two-step method. The thickness and length of the heat pipe are 3 mm and 200 cm, respectively. An experimental system was set up to measure the temperature distribution of heat pipes and calculate the thermal resistance by equation $R = \Delta T/Q$. At a same charge volume, the thermal resistance of heat pipe filled nano-fluid was lower than DI water.

Naphon et al. [10] Investigate experimentally the enhancement of heat pipe thermal efficiency with nanofluids is presented. The heat pipe is fabricated from the straight copper tube with the outer diameter and length of 15, 600 mm, respectively. The heat pipe with the de-ionic water, alcohol, and nanofluids (alcohol and nanoparticles) are tested. The titanium nanoparticles with diameter of 21 nm are used in the present study which the mixtures of alcohol and nanoparticles are prepared using an ultrasonic homogenizer. Effects of percentage charge amount of working fluid, heat pipe tilt angle and %nanoparticles volume concentrations on the thermal efficiency of heat pipe are considered. The nanoparticles have a significant effect on the enhancement of thermal efficiency of heat pipe. The thermal efficiency of heat pipe with the nanofluids is compared with that the based fluid.

Ming et al. [11] study the effect of magnetic fluid as the working fluid of the flat plate heat pipe. Flat plate heat pipe is one of the highly effective thermal spreaders. Magnetic fluid is liquid and can be moved by the force of magnetic field. Therefore, the magnetic fluid is suitable to be used as the working fluid of flat plate heat pipes which have a very small gap between evaporation and condensation surfaces. They

prepared a disk-shaped wickless flat plate heat pipe, and the distance between evaporation and condensation surfaces is only 1 mm. From experimental study, the magnetic fluid flat plate heat pipe can achieve more uniform heat flux distribution on the condensation surface than water flat plate heat pipe.

Kempers et al. [12] Study experimentally the effect of the number of mesh layers and amount of working fluid on the heat transfer performance of copper–water heat pipes with screen mesh wicks. For all orientations, the maximum heat transfer through the heat pipe increased as the number of mesh layers of the wick was increased, as expected. The heat pipes with amounts of working fluid close to that required to fully saturate the wick performed similarly. Jhan et al. [13] presents visualization and measurement of the evaporation resistance for operating flat-plate heat pipes with sintered multi-layer copper-mesh wick. Kaya et al. [14] developed a numerical model to simulate the transient performance characteristics of a loop heat pipe. Kang et al. [15] investigated experimentally, the performance of a conventional circular heat pipe provided with deep grooves using nanofluid. The nanofluid used in their study was aqueous solution of 35 nm diameter silver nano-particles. It is reported that, the thermal resistance decreased by 10-80% compared to that of pure water.

Pastukhov et al. [16] experimentally, investigated the performance of a loop heat pipe in which the heat sink was an external air-cooled radiator. The study showed that the use of additional active cooling in combination with loop heat pipe increases the value of dissipated heat up to 180 W and decreases the system thermal resistance down to 0.29 K/W. Chang et al. [17] investigated, experimentally, the thermal performance of a heat pipe cooling system with thermal resistance model. An experimental investigation of thermosyphon thermal performance consider water and dielectric heat transfer liquids as the working fluids was performed by Jouhara et al. [18]. The copper thermosyphon was 200 mm long with an inner diameter of 6 mm. Each thermosyphon was charged with 1.8 ml of working fluid and tested with an evaporator length of 40 mm and a condenser length of 60 mm. The thermal performance of the water charged thermosyphon is compared with the three other working fluids (FC-84, FC-77 and FC-3283). The parameters considered were the effective thermal resistance as well as the maximum heat transport. These fluids have the advantage of being dielectric which may be better suited for sensitive electronics cooling applications. Furthermore, they provide adequate thermal performance up to approximately 50 W, after which liquid entrainment compromises the thermosyphon performance.

Lips et al. [19] studied experimentally, the performance of plate heat pipe (FPHP). Temperature fields in the heat pipe were measured for different filling ratios, heat fluxes and vapor space thicknesses. Experimental results showed that the liquid distribution in the FPHP and consequently its thermal performance depends strongly on both the filling ratio and the vapor space thickness. A small vapor space thickness induces liquid retention and thus reduces the thermal resistance of the system. Nevertheless, the vapor space thickness influences the level of the meniscus curvature radii in the grooves and hence reduces the maximum capillary pressure. Thus, it must be, carefully, optimized to improve the performance of the FPHP. In all the cases, the optimum filling ratio obtained, was in the range of one to two times the total volume of the grooves. A theoretical approach, in non-working conditions, was

developed to model the distribution of the liquid inside the FPHP as a function of the filling ratio and the vapor space thickness.

Das et al. [20,21,24] and Lee et al. [23] found great enhancement of thermal conductivity (5-60%) over the volume fraction range of 0.1 to 5%.

All these features indicate the potential of nanofluids in applications involving heat removal. Issues, concerning stability of nanofluids, have to be addressed before they can be put to use. Ironically, nanofluids of oxide particles are more stable but less effective in enhancing thermal conductivity in comparison with nanofluids of metal particles.

The aim of the present work is to investigate, experimentally, the thermal performance of a heat pipe. The affecting parameters on thermal performance of heat pipe are studied. The type of working fluid (pure water and Al₂O₃-water based nanofluid), filling ratio of the working fluid, volume fraction of nano-particles in the base fluid, and heat input rate are considered as experimental parameters. Empirical correlation for heat pipe thermal performance, taking into account the various operating parameters, is presented.

EXPERIMENTAL SETUP AND PROCEDURE

A schematic layout of the experimental test rig is shown in Fig.1. This research adopts pure water and Al₂O₃-water based nanofluid as working fluids. The size of nano-particles is 40 nm. The test nanofluid is obtained by dispersing the nano-particles in pure water. The working fluid is charged through the charging line (7). In the heat pipe, heat is generated using an electric heater (2). The vapor generated in the evaporator section (11) is moved towards the condenser section (5) via an adiabatic tube (3) whose diameter and length are 27 mm and 150 mm, respectively. Both evaporator and condenser sections have the size of 27 mm-diameter and 90 mm-length. The condensate is allowed to return back to evaporator section by capillary action "wick structure" through the adiabatic tube. The surfaces of the evaporator section, adiabatic section, and condenser section sides are covered with 25 mm-thick glass wool insulation (4). Ten calibrated chromel-alumel thermocouples (K-type) are glued to the heat pipe surface (8) and distributed along its length to measure the local temperatures. All thermocouples are connected to a digital temperature recorder via a multi-point switch (9). The non condensable gases are evacuated by a vacuum pump. The heat pipe is evacuated to 0.01 bar via the vacuum line (10). The power supplied to the electric heater (1) is measured by a multi-meter. The input voltage was adjusted, using an autotransformer (1). The voltage drops across the heater were varied from 30 to 70 Volts. The A.C. voltage stabilizer is used to ensure that there is no voltage fluctuation during experiments. The pressure inside the evaporator was measured by a pressure gage with a resolution of 0.01 bar (6). An electric fan used for cooling the condenser section in forced convection but in natural convection the fan not used.

Thermocouples (with the uncertainty lower than 0.20 °C) are distributed along the surfaces of the heat pipe sections as follows: three thermocouples are attached to the evaporator section, four thermocouples are attached to the adiabatic section, and

three thermocouples are attached to the condenser section as shown in (Fig. 2). The obtained data for temperatures and input heat rate are used to calculate the thermal resistance. One can define the filling ratio, FR, as the volume of charged fluid to the total evaporator volume. The working fluid is charged at 30 °C. The effects of working fluid type, filling ratio, volume fraction of nano-particles in the base fluid, number of wick layers and heat input rate on the thermal performance of the heat pipe are investigated in the experimental work. The experimental runs are executed according to the following steps:

1. The heat pipe is evacuated and charged with a certain amount of working fluid
2. The supplied electrical power is adjusted manually at the desired rate using the autotransformer.
3. The steady state condition is achieved after, approximately, one hour of running time using necessary adjustments to the input heat rate. After reaching the steady state condition, the readings of thermocouples are recorded, sequentially, using the selector switch. The voltage of the heater is measured to determine the value of applied heat flux. Finally, the pressure inside the evaporator is recorded.
4. At the end of each run, power is changed and step 3 is repeated.
5. Steps 1 through 4 are repeated using with another adjusted amount of working fluid. The filling ratios, FR, used are 0.4, 0.60, 0.80, and 1.0.
6. Pure water and Al₂O₃-water based nanofluid are used as working fluids. Steps 1 through 5 are repeated for Al₂O₃-water based nanofluid using several values of volume fractions of nano-particles. The volume fractions used are 0.0%, 0.1%, 0.4%, 0.5%, 0.6%, 0.7%, 1.0%, and 1.5% respectively.
7. An Electric fan on for forced convection and off for natural convection.

DATA REDUCTION

Although heat pipes are very efficient heat transfer devices, they are subject to a number of heat transfer limitation. For high heat flux heat pipes operating in low to moderate temperature range, the capillary effect and boiling limits are commonly the dominant factor. For a given capillary wick structure and working fluid combination, the pumping ability of the capillary structure to provide the circulation for a given working fluid is limited. For operating the heat pipe, the maximum capillary pumping pressure, $\Delta P_{c,max}$ must be greater than the total pressure drop in the pipe,

$$\Delta P_{c,max} \geq \Delta P_f + \Delta P_v + \Delta P_g \quad (1)$$

Boiling limit is directly related to bubble formation in the liquid. In order that a bubble can exist and grow in liquid, a certain amount of superheat is required. Accurately characterizing the thermal power transfer, Q is a complicated task because it is difficult to accurately quantify the energy loss to the ambient surroundings. Therefore, the whole surface of the heat pipe is well insulated so that the rate of heat loss can be ignored. The heat input rate can be calculated using the supplied voltage and measured resistance such that,

$$Q = \frac{V^2}{r} \quad (2)$$

where V and r are the applied voltage in Volt and electric resistance of heater in Ohm, respectively.

The experimental determination of the thermal performance of the heat pipe requires accurate measurements of evaporator and condenser surface temperatures as well as the power transferred. Calculating evaporator and condenser temperatures is, relatively, a straightforward task. They are obtained by simply averaging the temperature measurements along the evaporator and condenser surfaces. Thus, evaporator and condenser temperatures can be expressed as:

$$\bar{T}_e = \frac{\sum_{i=1}^{i=N_e} T_{e_i}}{N_e}, \quad \bar{T}_c = \frac{\sum_{i=1}^{i=N_c} T_{c_i}}{N_c} \quad (3)$$

where N_e , N_c are the number of thermocouples on the evaporator and condenser, respectively. The obtained data for temperatures and heat input rate are then used to calculate the thermal resistance using the following relation,

$$R = \frac{(\bar{T}_e - \bar{T}_c)}{Q} \quad (4)$$

One can assume that the nano-particles are well dispersed within the base-fluid, so the effective physical properties are described by classical formulas which are mentioned by Das et al. [20] as;

$$\begin{aligned} \rho_{ef} &= (1 - \phi) \rho_m + \phi \rho_p \\ \rho_{ef} C_{p_{ef}} &= (1 - \phi) \rho_m C_{p_m} + \phi \rho_p C_{p_p} \end{aligned} \quad (5)$$

The effective dynamic viscosity of nanofluids can be calculated using different existing equations that have been obtained for two-phase mixtures. The following relation is the well-known Einstein's equation for a viscous fluid containing a dilute suspension of small, rigid, spherical particles,

$$\begin{aligned} \mu_{ef} &= \mu_m (1 + 2.5 \phi) \\ k_{ef} &= k_m (1 + 7.4 \phi) \end{aligned} \quad (6)$$

where, ϕ is the ratio of the volume of the nano-particle to the volume of the base fluid. The symbols K_m and Φ are the base fluid thermal conductivity and volume fraction of the nano-particle in the base fluid respectively.

The relevant thermo-physical properties of the solid nano-particles (Al_2O_3) used in the present study are $C_{p_p} = 773 \text{ J/kg.}^\circ\text{C}$, $\rho = 3880 \text{ kg/m}^3$, and $k_p = 36 \text{ W/m.}^\circ\text{C}$, which are mentioned in previous work [23].

One can calculate the reduction factor in total thermal resistance of heat pipe charged with nanofluid by referring its thermal resistance to that charged with pure water, expressed as;

$$RR = (R_m - R_{ef})/R_m \quad (7)$$

RESULT AND DISCUSSION

Experiments are performed on heat pipe considering two different working fluids; pure water and Al₂O₃-water based nanofluid. In both cases, the effect of heat input rate, Q , and filling ratio, FR on its performance are investigated. Moreover, in case of the nanofluid, the effect of varying volume fraction of the nano-particles in the base fluid, Φ , on the thermal performance of this heat pipe is also predicted. The values of local surface temperatures along all sections of the heat pipe are measured ($0 \leq X \leq 330$) mm, where X is measured from the beginning of the evaporator section. The range ($0.0 \leq X \leq 90$) mm represents the evaporator section, ($90 < X \leq 240$) mm represents the adiabatic section and ($240 \leq X \leq 330$) mm represents the condenser section.

Figure 3 illustrates the surface temperature along the heat pipe for natural and forced convection at heat input rate equal 8.2 W and filling ratio, $FR=0.4$ for different nanofluid concentration, and 3 wick layer. As expected, the surface temperature decreases with increasing the distance from the evaporator section due to the heat exchange between the heat pipe surface and working fluid. It is clear that the surface temperature decreases with increase of nano-particle concentration. As expected, the surface temperature decreases with increasing the distance from the evaporator along heat pipe. Figure (3-a) for natural convection and Figure (3-b) for forced convection, also we can find that the temperature of evaporator at forced convection is less than natural convection as shown in figures.

Figure 4 illustrates the variation of the total thermal resistance of the heat pipe, R with the Al₂O₃-water based nanofluid with different filling ratio for natural convection. As shown in the figure, R decreases with the increase of nanofluid concentration up to a value of nanofluid concentration equals to 0.6 %, after which R starts to increase with the increase of nanofluid concentration due to increasing of nanofluid inside evaporator. It can be also noticed that the thermal resistance, R is inversely proportional to number of wick layers for natural convection. Figure 5 illustrates the same variation as that of Fig. 4 for different nanofluid concentration for forced convection

The effect of adding nano-particles on the thermal performance of the heat pipe is more evident if the data is expressed as a plot of the reduction rate in total thermal resistance, RR versus nanofluid concentration, Φ , as shown in Fig. 6, i.e. the enhancement of thermal performance is increasing with the increase of nano-particles concentration. The addition of nano-particles has illustrated that during nucleate boiling some nano-particles deposit on the heated surface to form a porous layer. This layer improves the wet ability of the surface considerably. The thermal conductivity of the working fluid is also preferably high in order to minimize the temperature gradient.

The obtained heat transfer data is correlated as the following relation:

$$R = 0.594 \left[K_q^{-0.796} FR^{1.473} Pr^{-0.1532} \right] \quad (8)$$

The error in calculated thermal resistance is predicted by the above suggested correlation is around $\pm 5\%$, as shown in Fig. 7.

Figure 8 shows the variation of the total thermal resistance of the heat pipe, R with number of wicks. Generally, the thermal resistance decrease with increasing of number of wick layers.

Comparison with the Available Literature

Figure 9 shows a comparison between the present experimental results of the total resistance, R , using Al_2O_3 -water based nanofluid of $\Phi = 0.4\%$ to those reported by Lips and Lefèvre [19] who used a heat pipe charged with n- pentane nanofluid of $\Phi = 0.5\%$. One can see that the thermal resistance of the heat pipe decreases with increasing filling ratio up to a value of $\text{FR} = 0.45$, where it starts to increase with increasing the filling ratio. It can also observe that the present experimental results are, a little bit, lower than those reported by Lips et al [19], but they have the same trend. The discrepancies in both results may be due to the differences in dimensions of the tested heat pipes as well as due to the concentration of working fluids used.

CONCLUSIONS

Using heat pipes and based on the nanofluid literature, particularly those related to the optimum operating condition, the thermal performance enhancement of heat pipes charged with the nanofluid indicates the potential of the nanofluid use as substitute of conventional fluids. This finding makes the nanofluid more attractive as a cooling fluid for devices with high power intensity. A compact heat pipe is thermally tested with two different working fluids; pure water and Al_2O_3 -water based the nanofluid. The thermal performance of this heat pipe is predicted under different operating conditions including heat input rate, filling ratio, and wick type and volume fraction of the nano-particle in water. From the obtained data and its discussion, the following conclusions may be drawn:

- The optimum filling ratio of charged fluid in the tested heat pipe was about 0.4 to 0.50 for both pure water and Al_2O_3 -water based the nanofluid, respectively.
- By increasing concentration of the nanofluid, the thermal resistance of heat pipe can be decreased up to 0.4%.
- By increasing number of wick layer, the thermal resistance of heat pipe, also can be decreased.

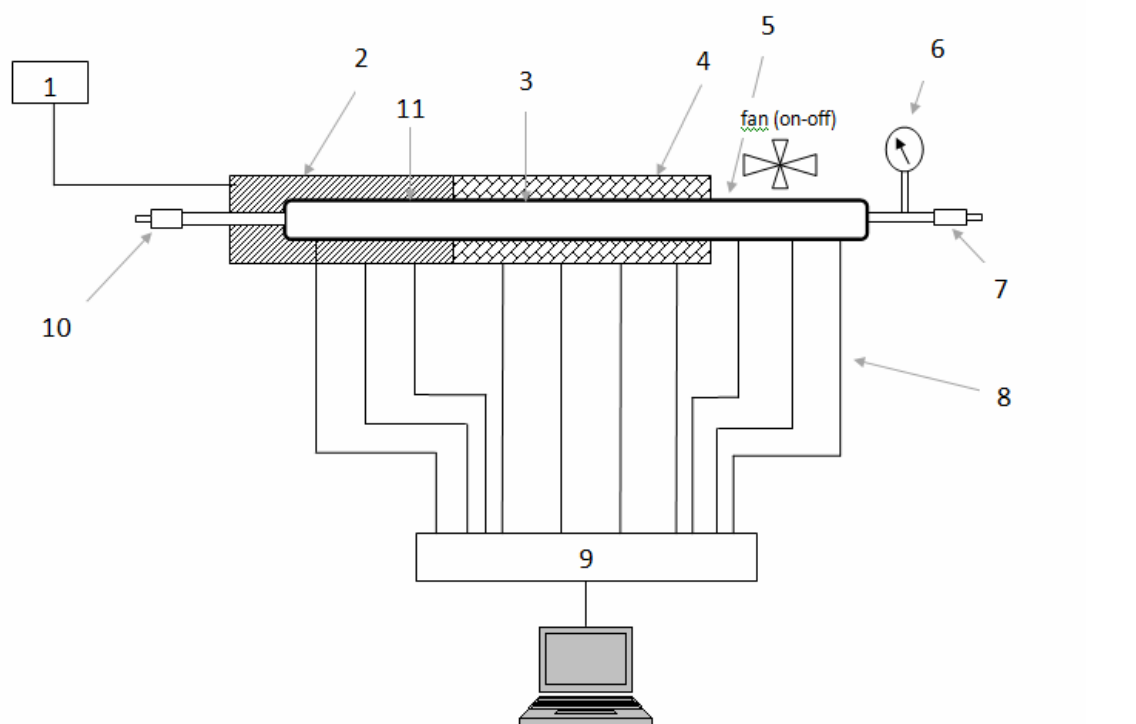
It can be said that better ability to manage thermal properties of working fluid translates into greater energy transport, smaller and lighter thermal systems. This may be applied to cooling of super computers, also cooling the core of nuclear reactors.

REFERENCES

- [1] Kyu Hyung Do , Hyo Jun Ha and Seok Pil Jang," Thermal resistance of screen mesh wick heat pipes using the water-based Al_2O_3 nanofluids", International Journal of Heat and Mass Transfer 53, pp. 5888–5894 (2010).

- [2] M.G. Mousa, "Effect of nanofluid concentration on the performance of circular heat pipe", *Ain Shams Engineering Journal* 2, pp. 63–69 (2011).
- [3] ZhenHua Liu, QunZhi Zhu, "Application of aqueous nanofluids in a horizontal mesh heat pipe", *Energy Conversion and Management* 52, pp. 292–300 (2011).
- [4] Maryam Shafahi, Vincenzo Bianco, Kambiz Vafai and Oronzio Manca, "An investigation of the thermal performance of cylindrical heat pipes using nanofluids", *International Journal of Heat and Mass Transfer*, 53, pp. 376–383 (2010).
- [5] R. Kempers, A.J. Robinson, D. Ewing and C.Y. Ching, "Characterization of evaporator and condenser thermal resistances of a screen mesh wicked heat pipe", *International Journal of Heat and Mass Transfer*, 51, pp. 6039–6046 (2008).
- [6] Zhen-Hua Liu, Yuan-Yang Li and Ran Bao, "Compositive effect of nanoparticle parameter on thermal performance of cylindrical micro-grooved heat pipe using nanofluids", *International Journal of Thermal Sciences*, 50, pp. 558-568 (2011).
- [7] S. Zeinali Heris, M. Nasr Esfahany and S.G. Etemad, "Experimental investigation of convective heat transfer of Al₂O₃/water nanofluid in circular tube", *International Journal of Heat and Fluid Flow*, 28, pp. 203–210 (2007).
- [8] Wei-Chiang Wei, Sheng-Hong Tsai, Shih-Yu Yang and Shung Wen Kanga, "Effect of Nanofluid on Heat Pipe Thermal Performance", *Heat Transfer, Thermal Engineering and Environment*, Corfu, Greece, August 20-22, pp.115-117 (2005).
- [9] Yu-Tang Chen, "Experimental Study of Silver Nanofluid on Flat Heat Pipe Thermal Performance", *Journal of Marine Science and Technology*, Vol. 18, No. 5, pp. 731-734 (2010).
- [10] Paisarn Naphon, Pichai Assadamongkol and Teerapong Borirak, "Experimental investigation of titanium nanofluids on the heat pipe thermal efficiency", *International Communications in Heat and Mass Transfer*, 35, pp. 1316–1319 (2008).
- [11] Zhang Ming, Liu Zhongliang, Ma Guoyuan and Cheng Shuiyuan, "The experimental study on flat plate heat pipe of magnetic working fluid", *Experimental Thermal and Fluid Science*, 33, pp. 1100–1105 (2009).
- [12] R. Kempers, D. Ewing and C.Y. Ching, "Effect of number of mesh layers and fluid loading on the performance of screen mesh wicked heat pipes", *Applied Thermal Engineering*, 26, pp. 589–595 (2006).
- [13] Jhan-Hong Liou, Chia-Wei Chang, Chi Chao and Shwin-Chung Wong, "Visualization and thermal resistance measurement for the sintered mesh-wick evaporator in operating flat-plate heat pipes", *international Journal of Heat and Mass Transfer*, 53, pp. 1498–1506 (2010).
- [14] Kaya, T., Pe´rez, R., Gregori, C. and Torres, A., "Numerical simulation of transient operation of loop heat pipes", *Applied Thermal Engineering*, vol.28, pp. 967-974 (2008).
- [15] Kang, S. W., Wei, W. C., Tsai, S. H., and Yang, S. Y., "Experimental investigation of silver nanofluid on heat pipe thermal performance", *Applied Thermal Engineering*, vol.26, pp. 2377–2382 (2006).

- [16] Pastukhov, V.G., Maidanik, Y. F., Vershinin, C.V., and Korukov, M.A., "Miniature loop heat pipes for electronics cooling", *Applied Thermal Engineering*, vol.23, pp. 1125-1135 (2000).
- [17] Chang,Y. W., Cheng, C. H., Wang, J. C., and Chen, S. L.," Heat pipe for cooling of electronic equipment", *Energy Conversion and Management*, (2008).
- [18] Jouhara¹, H., Martinet, O., Robinson, A.J., "Experimental Study of Small Diameter Thermosyphons Charged with Water", FC-84, FC-77 & FC-3283-5th European Thermal-Sciences Conference, Netherlands (2008).
- [19] Lips, S., Lefèvre, F., and Bonjou, J., "Combined effects of the filling ratio and the vapour space thickness on the performance of a flat plate heat pipe", *International Journal of Heat and Mass Transfer*, vol. 53, pp. 694–702 (2010).
- [20] Das, S. K., Choi, U.S., Yu,W., and Pradeep, T., "Nanofluid Science and Technology", Wily-Interscience (2007).
- [21] Das, S. K., Putra, N., Thiesen, P., and Roetzel, W., "Temperature dependence of thermal conductivity enhancement for nanofluids", *J. Heat Transfer*, vol.125, pp. 567-574 (2003).
- [22] Mansour, R.B., Galanis, N., and Nguyen, C.T., "Effect of uncertainties in physical properties on forced convection heat transfer with nanofluids," *Applied Thermal Engineering*, Vol. 27, pp. 240–249 (2007).
- [23] Lee, S., Choi, S.U.S, Li., S., and Eastman, J.A., "Measuring thermal conductivity of fluids containing oxide nanoparticles", *J. Heat Transfer*, vol. 121, pp. 280-289 (1999).
- [24] Das, S. K., Choi, U.S., Yu,W.,and Pradeep, T., "Nano Fluid Science and Technology", Wily-Interscience (2007).



- | | | | | |
|-------------------------------------|--------------------|------------------|----------------------|-----------------------|
| 1-power supply and auto transformer | 2- Electric heater | 3-Adiabatic sec. | 4-Insulation | 5-Condenser sec. |
| 6-Pressure gage | 7-Charge line | 8-Thermocouples | 9-Multi-point switch | 10-Vacuum line switch |
| 11- Evaporator sec. | | | | |

Fig.1. Schematic layout of the test rig.

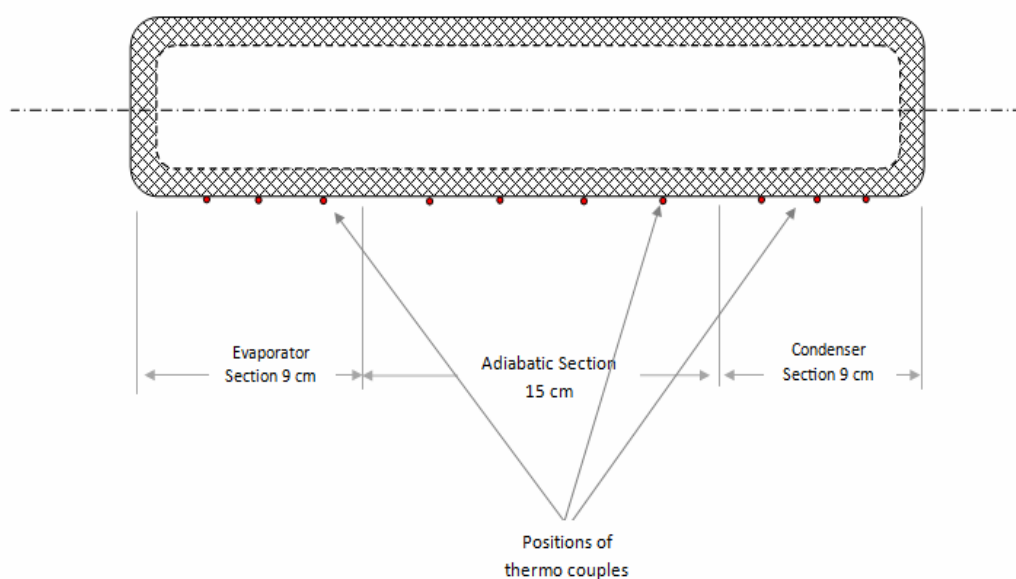


Fig. 2. Schematic layout thermocouples positions along the heat pipe.

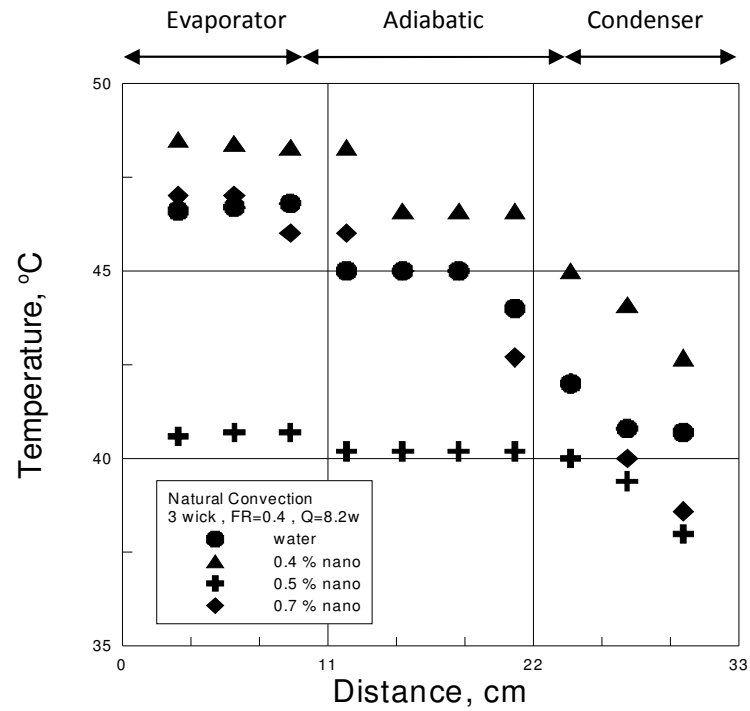


Fig. 3-a. Temperature distribution for natural convection.

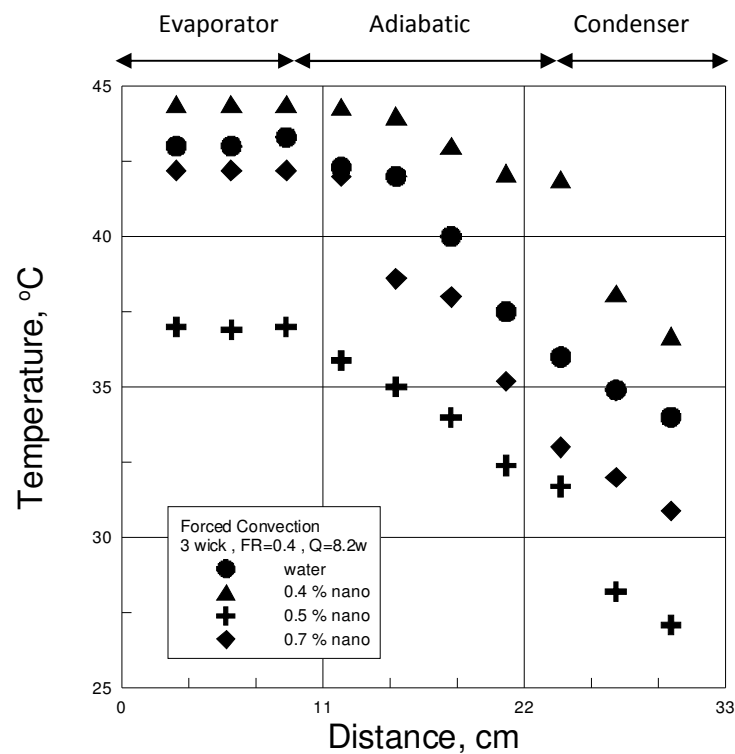


Fig. 3-b. Temperature distribution for forced convection.

Fig.3. Temperature distribution along the heat pipe surface for different nanofluid concentration.

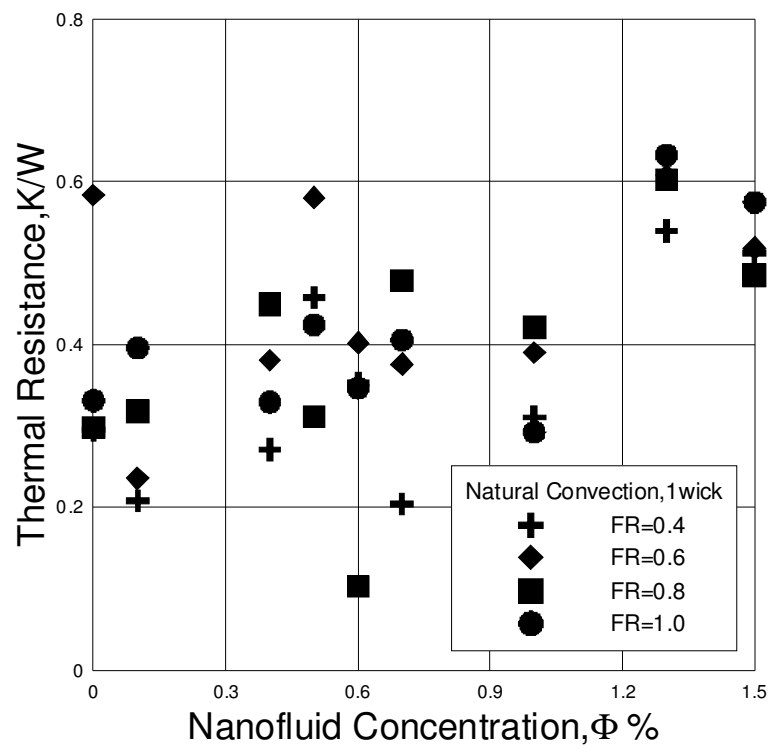


Fig. 4-a. Performance of heat pipe with using one wick.

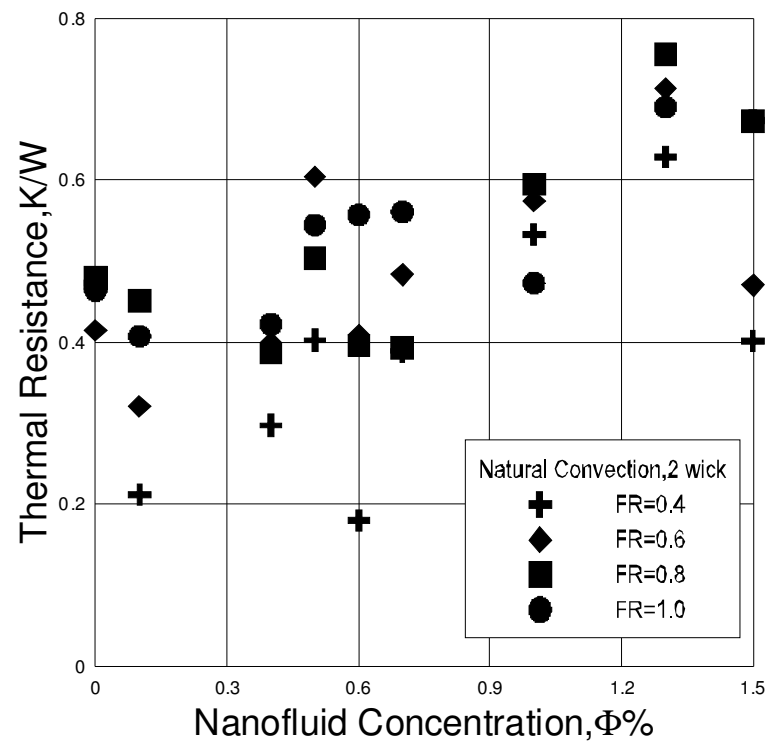


Fig. 4-b. Performance of heat pipe with using 2 wicks.

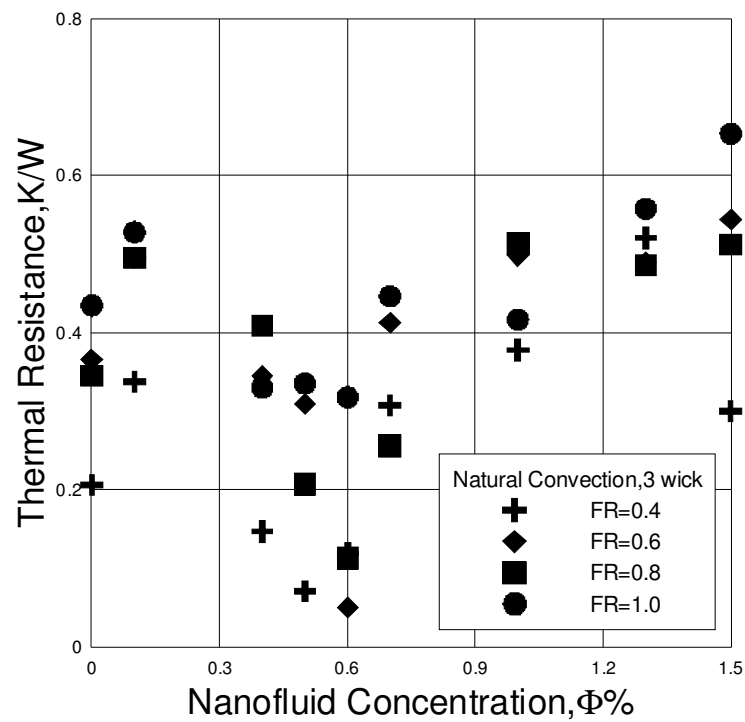


Fig. 4-c. Performance of heat pipe with using 3 wicks.

Fig.4. Average thermal resistance of heat pipe with different nanofluid concentration, natural convection.

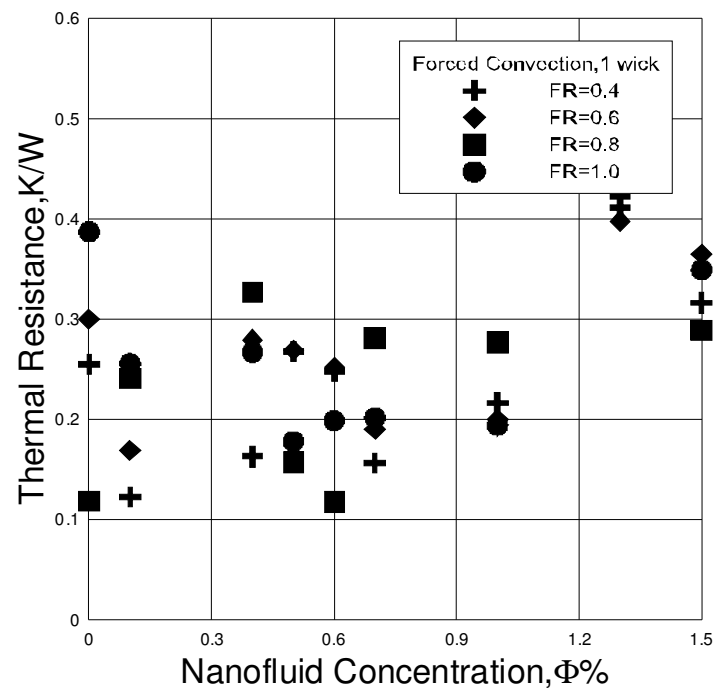


Fig. 5-a. Performance of heat pipe with using one wick.

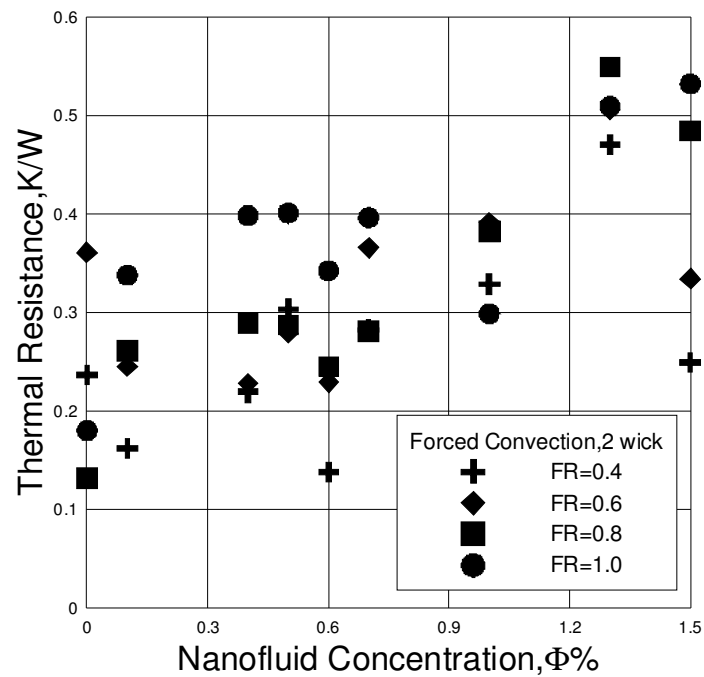


Fig. 5-b. Performance of heat pipe with using 2 wicks.

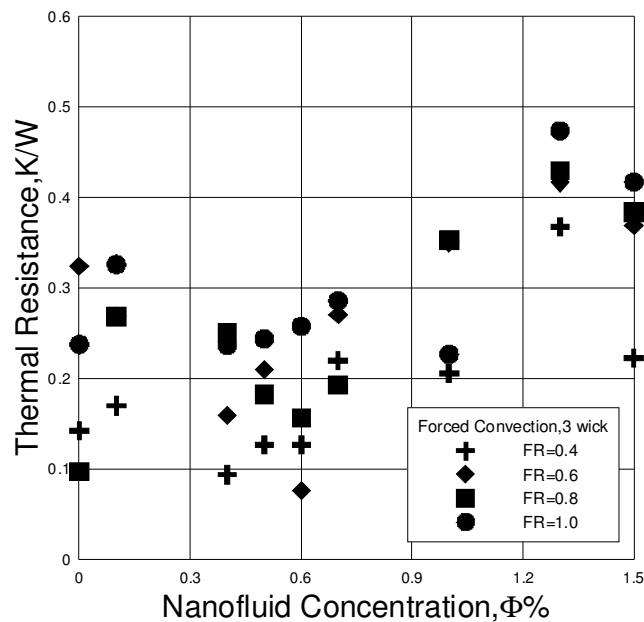


Fig. 5-c. Performance of heat pipe with using 3 wicks.

Fig. 5. Average thermal resistance of heat pipe with different nanofluid concentration, forced convection.

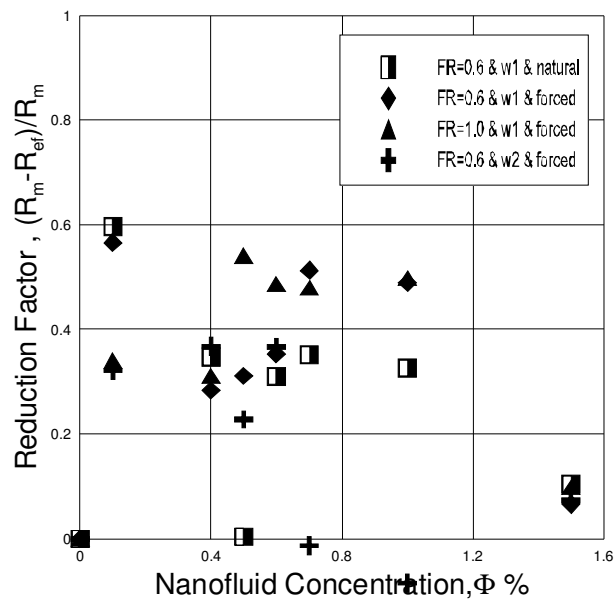


Fig. 6. Experimental reductions on thermal resistances versus nanofluid concentration over the tested range of heat input rate.

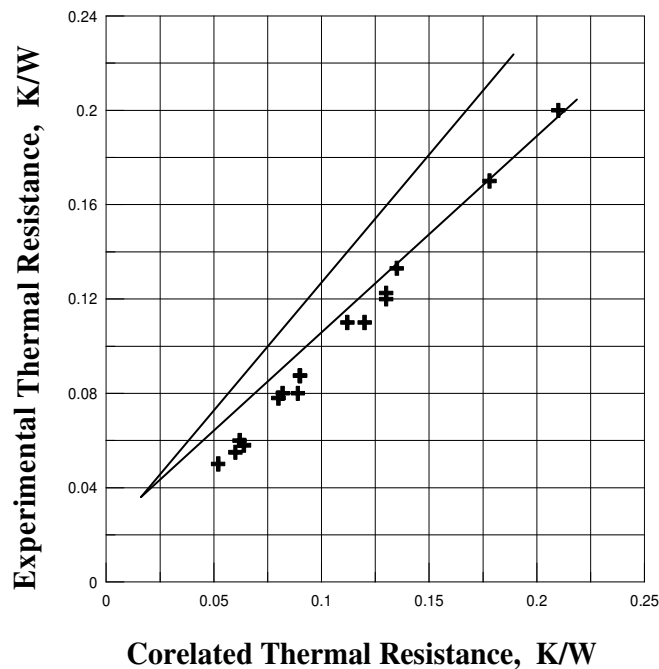


Fig.7. Experimental Thermal resistance versus correlated Thermal resistance over the tested range of heat input rate.

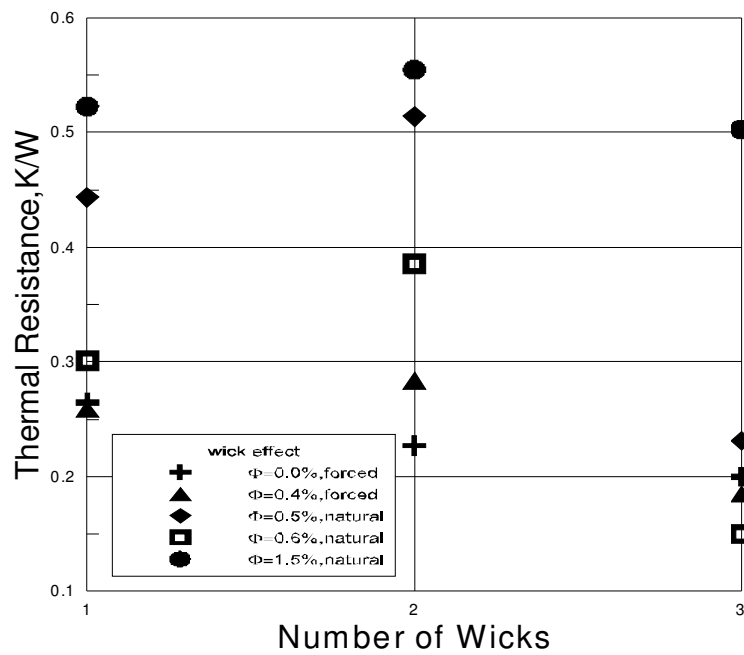


Fig. 8. Variation of thermal resistance with number of wicks.

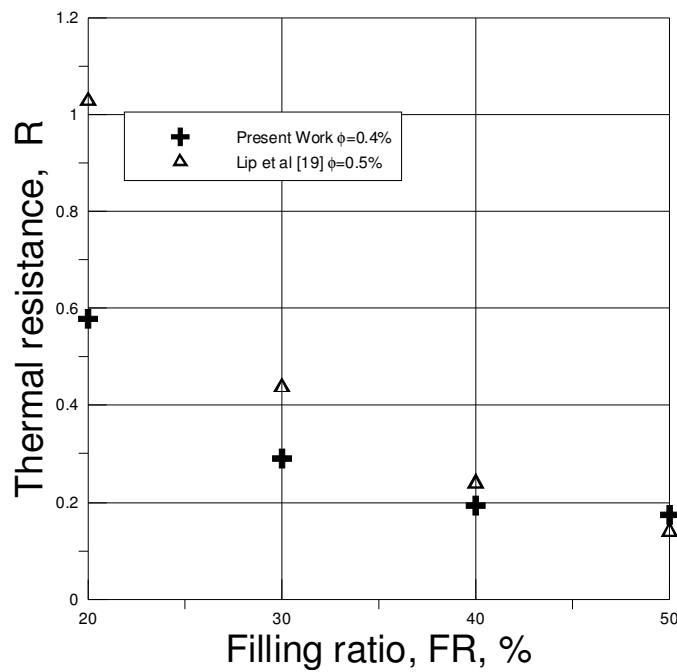


Fig. 9. Comparison between present data and previous one for the variation of thermal resistance.